University of Nebraska - Lincoln

DigitalCommons@University of Nebraska - Lincoln

Biological Systems Engineering: Papers and Publications

Biological Systems Engineering

2014

Alginate/silica hybrid materials for immobilization of green microalgae *Chlorella vulgaris* for cellbased sensor arrays

Angela K. Pannier
University of Nebraska-Lincoln, apannier2@unl.edu

Ulrich Soltmann
GMBU e.V., Department of Functional Coatings, D-01317 Dresden, Germany

Bettina Soltmann
Institute of Materials Science and Max Bergmann Center of Biomaterials, TU Dresden, D-01062 Dresden, Germany

Rolf Altenburger
UFZ Helmholtz Centre for Environmental Research, Department Bioanalytical Ecotoxicology, D-04318 Leipzig, Germany

Mechthild Schmitt-Jansen
UFZ Helmholtz Centre for Environmental Research, Department Bioanalytical Ecotoxicology, D-04318 Leipzig, Germany

Follow this and additional works at: https://digitalcommons.unl.edu/biosysengfacpub

Part of the Bioresource and Agricultural Engineering Commons, Environmental Engineering Commons, and the Other Civil and Environmental Engineering Commons

PAPER

Alginate/silica hybrid materials for immobilization of green microalgae *Chlorella vulgaris* for cell-based sensor arrays†

Angela Pannier,*[a] Ulrich Soltmann,[a] Bettina Soltmann,[b] Rolf Altenburger[c] and Mechthild Schmitt-Jansen[c]

Thin layers and patterned dot arrays of sodium alginate containing living microalgal cells were deposited onto glass carriers which were subsequently gelled using amino-functionalized silica sol to obtain reinforced alginate hydrogels. The resulting alginate/silica hybrid materials showed improved stability in salt-containing solutions compared to alginate gels gelled by traditional methods using Ca^{2+}-ions. Cell arrays were patterned by printing nanolitre-scale drops of sodium alginate/cell suspension using a non-contact micro-dosage system which allows the printing of solutions of high viscosity. Cultures of the green microalga *Chlorella vulgaris* were immobilized within the newly developed alginate/silica hydrogels in order to demonstrate the potential of the hybrid matrix for the design of cell-based detection systems. The herbicide atrazine as well as copper ions have been used as model toxicants. Short-term toxicity tests (exposure time: 1 h) have been carried out using atrazine and changes in chlorophyll *a* (Chl *a*) fluorescence were measured by imaging pulse amplitude modulated-fluorometry (Imaging-PAM). *C. vulgaris* cells immobilized within alginate/silica hydrogels demonstrated a highly reproducible response pattern and compared well to freely suspended cells. Activity and response sensitivity of immobilized cells to atrazine was largely maintained for up to 8 weeks, especially when stored under cool conditions in the dark. Furthermore, immobilized cells could be repeatedly used for short-term toxicity tests as atrazine produces a reversible inhibition of photosynthesis.

Introduction

Immobilizing living cells within defined cell arrays on platforms such as biochips or optic fibres holds much promise in miniaturizing toxicity test systems for rapid and parallel measurements of samples in mass scale. Monitoring the response of several species and/or multiple strains to different stressors simultaneously in a single device could provide a valuable tool to not only detect toxic effects but also to identify specific toxicants or classes of toxicants. For instance Podola *et al.*[1] demonstrated that the identification of a specific herbicide is in principle possible by employing an array chip algal biosensor based on nine different microalgal strains. Altamirano *et al.*[2] and Peña-Vázquez *et al.*[3] further suggested the use of mutants

sensitive/resistant to a given toxicant to further increase the sensitivity and to improve the specificity of response patterns.

During the last years, advances in cell immobilization strategies have provided the possibility to position different cells in microarrays by using various deposition and printing techniques,[4,5] such as micro-contact printing (micro-stamping)[6,7] and non-contact printing like ink-jet printing.[8–12] However, immobilization of living cells is still a crucial step as the viability and activity of the cells has to be maintained by ensuring a firm fixation of immobilized cells at the same time.

The sol–gel process holds much promise to design cell-based detection systems and firmly attach cells within mechanically and chemically stable silica gels.[13] A few studies exist where microarrays of silica gels were directly printed to immobilize proteins[14–17] and even living cells.[18,19] Nevertheless, it has been shown that pin printing is difficult to perform using traditional sol–gel processing solutions[14] due to severe deposition problems. Once the silica sol is neutralized, the polymerization reaction (condensation) is accelerated, which results in an increasing viscosity during the printing process. In order to preserve spot uniformity and to avoid clogging of the pin, specific care has to be taken that the gelation reaction does not occur too quickly so that viscosity changes of the spotting solution can be minimized during the printing process.[19,20]

[a]GMBU e.V., Department of Functional Coatings, D-01317 Dresden, Germany. E-mail: pannier@gmbu.de; Fax: +49 0351 2695 341; Tel: +49 0351 2695 342

[b]Institute of Materials Science and Max Bergmann Center of Biomaterials, TU Dresden, D-01062 Dresden, Germany

[c]UFZ Helmholtz Centre for Environmental Research, Department Bioanalytical Ecotoxicology, D-04318 Leipzig, Germany

† Electronic supplementary information (ESI) available. See DOI: 10.1039/c4tb00944d

However, when choosing prolonged gelation times, detrimental effects on spotted cells may arise during gelation as living cells are susceptible to drying-out. To minimize drying-out, Ge et al.[19] performed gelation of printed silica gel spots in a humid atmosphere, and after 30 min of gelling, cell arrays were immediately transferred to aqueous media.

In the present study, an alginate/silica hybrid gel was applied in order to circumvent printing and drying problems. The anionic polysaccharide alginate was chosen due to its good applicability to printing techniques, transparency, and good biocompatibility.[21–23] Arrays of alginate with embedded cells can easily be deposited onto solid supports by printing nanolitre-scale drops of sodium alginate/cell suspensions with no expectable viscosity changes. Directly after printing, the sodium alginate dots were gelled using amino-functionalized silica sol to obtain alginate/silica hydrogels. After that, gelled dots were immediately washed and transferred to fresh media. In this way, alginate dots were in liquid media all the time except during the printing process which, however, takes only a few seconds.

Furthermore, by the combination of negatively charged sodium alginate with positively charged amino-groups of the amino-functionalized silica sol a hybrid gel is formed which exhibits a good chemical stability in biological buffer or nutrient solutions. In contrast, alginate gels commonly gelled using divalent cations such as calcium (Ca^{2+}) which has been, by far, the most studied cross-linker of alginate[24] often show insufficient stability in such solutions. Ca^{2+}-ions are easily removed by chelating agents (e.g., phosphates and citrates) and monovalent ions such as Na^+ and K^+, as found in usual biological buffers and media.[22,24,25] Thereby the cross-linking of the Ca–alginate gel is decreased, which results in destabilization of the alginate matrix. This causes osmotic swelling of the gel matrix leading to leakage of the immobilized cells and even to the complete disintegration of the alginate gel network. Thus, pure Ca–alginate carriers cannot be maintained for longer periods in aqueous solutions.[24,25]

Several strategies have been explored to increase the stability of the alginate matrix, such as the use of divalent cations other than Ca^{2+} for cross-linking (e.g., Ba^{2+} or Sr^{2+})[22] or reinforcement by additional cross-linking using polycations, such as poly-L-lysine or poly(ethyleneimine).[26,27]

The sol–gel process has shown to be a promising approach to prepare reinforced alginate/silica hybrid materials.[24,28] Combining alginate with inorganic silica matrices offers several advantages in that the resulting ceramic-like silica matrices possess high mechanical and chemical stability. Existing attempts to combine the benefits of the sol–gel process and alginate gels have recently been described by Coradin et al.[24] For instance, silica sols were mixed with a solution of sodium alginate followed by gelation with Ca^{2+}.[29] Another strategy relies on the pre-immobilization of the cells within Ca^{2+}-cross-linked alginate beads followed by reinforcement either by embedding the Ca–alginate beads within thick silica gel bodies[25,30,31] or by silica layer deposition at the bead surface.[32,33] When silica is deposited onto alginate, it is important to note that silica and alginate are both negatively charged at neutral pH; only weak hydrogen bonds may arise between the two components.[24] To strengthen the interface between alginate and silica, Coradin et al.[32] deposited an intermediate layer of polycations (e.g., poly-L-lysine) on the Ca–alginate bead surface, resulting in a net positive charge favouring silica condensation at the surface of the Ca–alginate matrix. Sakai et al.[33] further improved the silica layer deposition by using an amino-functionalized silica alkoxide: aminopropyl-trimethoxysilane. The organically modified silica alkoxide bearing cationic groups was used alone or in combination with the non-modified silica precursor tetramethoxysilane (TMOS). Ammonium moieties of the amino-functionalized silica sol (aminosilane) interacted with the anionic groups of the alginate. In this way, silica layers were directly deposited onto Ca–alginate without requiring an intermediate layer. Kurayama et al.[34] have shown that not only a silica layer is formed at the surface of alginate beads previously gelled using Ca^{2+}-ions but that the amino-functionalized silica nanoparticles are able to penetrate into the polymeric network of Ca–alginate and replace the Ca^{2+} ions.

In the present study, the possibility to directly solidify sodium alginate with amino-functionalized silica sols without the previous gelation by calcium salt was investigated to reduce preparation steps on one hand and to avoid the presence of Ca^{2+} ions on the other hand as calcium is implicated in various signalling pathways and its presence may lead to biological interference in some test systems.[19]

The applicability of alginate/silica hydrogels as immobilization matrix to design cell-based detection systems for toxicity responses was investigated using cultures of the green microalga Chlorella vulgaris as sensing microorganisms. Microalgae are frequently used in bioassays as they are very sensitive towards different pollutants[35] such as heavy metals[36–38] and herbicides.[3,30,39]

In the present study, the triazine herbicide atrazine was used as model substrate for short-term toxicity testing in aquatic samples. The phytotoxic action of this herbicide is based on the interference with the electron transport in the photosystem II (PSII) of photosynthetic organisms.[40] For quantification of the resulting changes in photosynthetic activity, variable chlorophyll a (Chl a) fluorescence was used as a rapid and sensitive indicator.[41] Chl a fluorescence can easily be monitored using non-invasive methods such as fluorescence spectroscopy[36] and pulse amplitude modulated (PAM) fluorometry.[38,41,42] As these methods are non-invasive, they provide the possibility to use immobilized cells repeatedly for toxicity assessment after cell recovery. In this way, long-term maintenance of activity and response sensitivity during storage and repeated usage of C. vulgaris cells immobilized within alginate/silica hydrogels were investigated over a period of eight weeks. Imaging-PAM fluorometry based on the saturation pulse method[42] was applied to quantify the changes in photosynthetic activity due to the presence of atrazine during short-term toxicity tests (exposure time: 1 h).

Experimental section

Chemicals

Sodium alginate (viscosity of 1% solution in water at 20 °C: 350–550 Pa s) was purchased from Roth (Karlsruhe, Germany).

The diamino-functional silane *N*-(2-aminoethyl)-3-amino-propyltrimethoxysilane (CAS RN 1760-24-3) was obtained from ABCR (Karlsruhe, Germany) and the silica precursor tetraethoxysilane (TEOS; CAS RN 78-10-4) from Wacker Chemie GmbH (Munich, Germany).

The cationic polyamine solution Catiofast 159 used for surface-modification of glass was purchased from BASF (Ludwigshafen, Germany).

The herbicide atrazine (CAS RN 1912-24-9) was supplied by Riedel deHaën (Seelze, Germany) with a purity of >99%. The solvent dimethyl sulfoxide (DMSO; CAS RN 67-68-5) was purchased from Merck (Darmstadt, Germany).

De-ionized water (dI-H_2O), obtained from a SERADEST S600 system (<0.5 $\mu S\ cm^{-1}$ conductivity; USF GmbH, Ransbach-Baumbach, Germany), was used for the preparation of various solutions.

Microalgal strain and culture conditions

The unicellular freshwater green algae *Chlorella vulgaris* strain C1 (IPPAS C-1, Moscow, Russia) were maintained as batch cultures on an inorganic medium (1/2 Tamiya medium,[43] pH 5.5–6.0, composition see ESI, Table 1†) at 25 °C under constant illumination (25 μmol photons per $m^2\ s^1$) and bubbling with ambient air. Culture media were exchanged weekly.

Surface modification of glass carriers

Standard microscopic glass slides (SuperFrost® cut edges, Menzel GmbH, Braunschweig, Germany) as well as glass discs (1.5 cm diameter, Marienfeld GmbH, Lauda-Königshofen, Germany) fitting into 24-well plates were used as carrier substrate for cell immobilization. To obtain stable adhesion of negatively charged alginate gels, the glass surface was modified by cationic coating. The glass was cleaned with HNO_3 (2%) and aqua dest (three times). After drying, glass slides were activated by microwave plasma activation using Creaetch 250 Plasma MV (Creavac GmbH) and dip coated using a 0.5% polycation solution Catiofast 159, directly after activation. Coated glass slides were finally air dried and autoclaved at 121 °C for 15 minutes. The cationically modified glass slides were storable under dry conditions for several months prior to further usage.

Synthesis of amino-functionalized silica sol

Amino-functionalized silica sols were prepared by mixing the silica precursor tetraethoxysilane (TEOS), and the diamino-functional silane, *N*-(2-aminoethyl)-3-aminopropyltrimethoxysilane with de-ionized water and 1 *N* HCl; in a ratio (v/v) of 1 : 2 : 17 : 6 respectively. The mixture was stirred overnight at room temperature to ensure hydrolysis. Alcohol formed during hydrolysis was removed by evaporation. Due to the preparation conditions of the amino-functionalized silica sol, no further sterilization was necessary to use it for the immobilization experiments.

Particle size distribution of formed silica nanoparticles were investigated at 25 °C by dynamic light scattering using Zetasizer 1000HSA (Malvern Instruments).

Prior to cell encapsulation, the pH of the amino-functionalized silica sols was adjusted to pH 7.5 by using 30% HCl.

Deposition of sodium alginate containing *C. vulgaris* cells

As sodium alginate is not heat stable, a solution of sodium alginate (2%, w/v) was prepared shortly before cell immobilization under semi-sterile conditions by dissolving 1 g of sodium alginate within 50 mL of sterile de-ionized water.

C. vulgaris cells were harvested and cell density was determined using a microscope counting chamber (Neubauer chamber, depth 0.1 mm). Cells were precipitated by centrifugation at 4000 rpm (= 2800g) and diluted with 2% sodium alginate (w/v) to a density of 10^8 cells per mL. The suspension of *C. vulgaris* cells and sodium alginate was deposited onto surface-modified glass slides within dot arrays or thin films by the procedures described below. Subsequently, the deposited sodium alginate was gelled by amino-functionalized silica sol or Ca^{2+}-ions.

Printing of single dot arrays. Arrays of single dots of the suspension of *C. vulgaris* cells and sodium alginate were spotted onto surface-modified glass using a non-contact piezoelectric micro-dosage printer Nano-Plotter 2.0 (Gesellschaft für Silizium-Microsysteme, GeSiM, Großerkmannsdorf, Germany) (for details see Gepp *et al.*[44]). The micro-dosage system was equipped with a modified micrometering valve (Delo-Dot, DELO Industrial Adhesives GmbH, Windach, Germany) allowing dispensing microvolumes of the highly viscous sodium alginate solution. Dots were dispensed in an array of 5 × 5 dots with a center-to-center spacing of 1000 μm. The volume of one droplet was 70 nL (corresponding to about 7 × 10^3 cells) resulting in a diameter of about 650 ± 30 μm per dot onto Catiofast 159-modified glass slides. Due to the high viscosity of the sodium alginate, cells remained evenly distributed within the printing solution during the printing process.

To prevent drying, air humidity was maintained between 70% and 80% within the printing chamber. The time required for printing an array of 5 × 5 dots was in the order of 1 s. Immediately after spotting, dots of sodium alginate were gelled by incubation in neutralized amino-functionalized silica sol or by cross-linking using traditional Ca^{2+}-ions (see below).

Dip coating of thin films. Surface-modified glass was dipped into a suspension of 2% sodium alginate containing *C. vulgaris* cells. Due to the high viscosity of the sodium alginate and its resulting low drain-off characteristics, it was necessary to subsequently centrifuge the samples at 1000 rpm (= 176g) for 15 s to obtain homogenous, thin films. Immediately after centrifugation, the films of sodium alginate were gelled by the procedures described below.

Gelation of the deposited sodium alginate

Alginate/silica hydrogels (gelation by amino-functionalized silica sol). The arrays of sodium alginate dots were gelled by incubation in neutralized amino-functionalized silica sol for 5 s. Thin films were gelled for 2 min. The obtained alginate/silica hydrogels were further washed with de-ionized water and

transferred into fresh culture media (1/2 Tamiya) until further use.

Ca–alginate hydrogels (gelation by traditional calcium-ions). For comparison of matrix performance and stability, sodium alginate deposited onto surface-modified glass slides was ionically cross-linked using 0.1 M CaCl$_2$ solution (20 min incubation). Ca–alginate hydrogels were washed using de-ionized water and further treated in the same way as alginate/silica hydrogels.

Characterization of alginate/silica hydrogels

Characterization of chemical composition. Chemical composition of alginate/silica hydrogels containing no cells were characterized by energy dispersive X-ray (EDX) analysis and Fourier transform infrared (FT-IR) spectroscopy.

The inner and outer surface of freeze-dried alginate/silica films (gelation time 2 min) were characterized by EDX analysis using SwiftED-TM detector (Oxford Instruments) integrated into a scanning electron microscope (SEM) Hitachi Tabletop Microscope TM-1000 (Hitachi High Technologies). Detectable elements range from Na(11) to U(92). For FT-IR spectroscopy, KBr pellets of sodium alginate, Ca–alginate and alginate/silica hydrogels (gelation time 1.5 h) were prepared and FT-IR transmission spectra were recorded using Bruker Alpha spectrometer (Bruker Corporation) (scan numbers: 64; resolution: 4 cm^{-1}).

Stability testing. The adhesion properties of alginate dots and thin layers onto surface-modified glass slides have been investigated in de-ionized water with and without stirring at 1000 rpm for up to three months.

Furthermore, the stability of alginate/silica as well as Ca–alginate micro-arrays printed onto Catiofast 159 coated glass slides was tested in different solutions (de-ionized water, 0.9% NaCl, 0.1 M phosphate buffer pH 7.0, and 1/2 Tamiya medium). Alginate arrays were characterized by visual observation and microscopic study.

Characterization of immobilized cells by microscopy

C. vulgaris cells were immobilized within Ca–alginate as well as alginate/silica hydrogels and cultured within 1/2 Tamiya medium at 20 °C under daylight. Immobilized cell cultures were monitored *via* light microscopy and fluorescence microscopy using Olympus BX60 (Olympus, Hamburg, Germany) equipped with a CCD camera (CC-12, Olympus Soft Imaging System, Hamburg, Germany). The following filters were used for the observation of the Chl *a* fluorescence: Olympus WB (excitation bandpass 460–490 nm, beam splitter 500 nm, emission filter 520 nm) and Olympus NUA (excitation bandpass 360–370 nm, beam splitter 400 nm, emission filter 420–460 nm). Exposure times were chosen in order to obtain a good contrast ratio. Images were captured using the computer program Cell-A (Olympus, Hamburg, Germany).

Initial toxicity testing using fluorescence microscopy

Changes in Chl *a* fluorescence were investigated using copper-ions as model toxicant. Dot arrays of alginate/silica hydrogels containing *C. vulgaris* cells were incubated in 1/2 Tamiya

medium containing 2 mmol copper nitrate. A control sample not containing Cu was included. At specific time intervals (0.5 h to 5 h) fluorescence images of individual dots were taken (Filter characteristics: Ex.: 460–490 nm; Em. > 520 nm; shutter speed 100 ms).

Toxicity testing using PAM fluorometry

Short-term toxicity tests of photosynthesis inhibition. Glass discs (1.5 mm diameter) containing *C. vulgaris* cells immobilized within thin layers of alginate/silica gels were placed into 24-well plates (Greiner GmbH, Frickenhausen, Germany) and 2 mL of fresh culture media (1/2 Tamiya) were added into each well. The stock solution of the herbicide atrazine (10 g L^{-1} in dimethyl sulfoxide DMSO) was diluted in DMSO and added to the samples in six different concentrations ranging from 0.002 mg L^{-1} to 10 mg L^{-1}. Samples containing the equal amount of DMSO as the treatments (0.1%) and further samples without any addition served as controls. Each concentration was tested in triplicate. Samples were exposed to the herbicide on a shaker (100 rpm) under continuous light conditions having a light intensity of about 40 μmol photons per m^2 s^1, at about 20 °C before Chl *a* fluorescence measurements. If not specifically mentioned, duration time of exposure to atrazine was 1 h.

Fluorescence quenching analysis of chlorophyll *a*. Chl *a* fluorescence measurements were conducted at two random points on each disc using an Imaging-PAM chlorophyll fluorometer (Maxi-Imaging-PAM, Walz, Effeltrich, Germany). Before starting measurements, samples were kept in the dark for 10 min to ensure that all reaction centers of the PSII were open. After dark adaptation, the maximum quantum yield of electron transport of PSII, $Y(I)$, was measured by the saturating pulse method (for details see Schreiber *et al.*[42]) and calculated according to Genty *et al.*[45] and Kromkamp and Förster[46] with eqn (1).

$$Y(I) = \Delta F/F_{max} = (F_{max} - F)/F_{max} \qquad (1)$$

where, the maximum fluorescence yield (F_{max}) was measured at a wavelength >630 nm during a saturating pulse (instrumental settings: excitation 450 nm, duration 800 ms, intensity 5, gain 2) which leads to the closure of all PSII reaction centers and the full inhibition of energy conversion. Saturation pulses were conducted with F_{max} measurement intervals of 2.5 minutes. The momentary fluorescence yield (F) was determined between the saturation pulses. The percentage to which the photosynthesis efficiency was inhibited was calculated based on three measurements.

The relative inhibition of variable fluorescence in relation to controls was calculated by comparing the quantum yield without ($Y(I)_{control}$) and with addition of atrazine ($Y(I)_{sample}$) according to eqn (2).

$$\text{Inhibition [\%]} = 100 \times (1 - Y(I)_{sample}/Y(I)_{control}) \qquad (2)$$

Inhibition data ($N = 6$) were used to model concentration–response curves using log–logistic analysis according eqn (3).

$$y = A_{min} + ((A_{max} - A_{min})/(1 + x/x_0)^p) \qquad (3)$$

where y is the effect and A_{min} and A_{max} refers to the minimal and maximal response, x is the concentration, x_0 the concentration at median efficacy and p stands for the slope. After data inspection, A_{min} was fixed to 0, while A_{max} was kept variable. Estimation of statistical parameters was performed using non-linear regression and least square fitting of the software Origin 8.1 (OriginLap, Northampton, MA, USA). The median effect concentration (EC_{50}) which corresponds to 50 % inhibition of photosynthesis was calculated (see ESI, Tables 2–5†).

Evaluation of sensitivities of immobilized *versus* suspended cells. Short-term toxicity tests were carried out using freely suspended *C. vulgaris* cells (at a density of 10^6 algal cells per mL) as well as immobilized cells coated onto glass discs within alginate/silica hydrogels. Samples were exposed to atrazine under continuous light and agitation, as described previously. Fluorescence quenching analysis of Chl *a* was performed after 1 h, 3 h, 5 h and 24 h exposure to the herbicide atrazine. Values after 24 h exposure were obtained after conduction of a light/dark period of 14/10 h.

Evaluation of reproducibility. Samples of *C. vulgaris* cells were cultured and harvested for immobilization at four independent points of time – over a period of two months. For evaluation of sensitivities of these four independent batches, toxicity tests were conducted shortly after immobilization. Samples in each batch were tested in duplicates.

Evaluation of storage stability. Directly after immobilization, coated glass discs were placed in 24-well plates containing 2 mL culture media (1/2 Tamiya). Subsequently, samples were either stored at 4 °C in the dark or at 20 °C under a light/dark cycle of 14/10 h and an irradiance of about 40 μmol photons per m^2 s. Latter samples were shaken at 100 rpm and nutrient media were exchanged daily to avoid nutrient depletion. After specific periods of storage (1, 2, 4 and 8 weeks), samples were washed three times with fresh culture media and toxicity tests (exposure time: 1 h) were conducted according to the method described above.

Evaluation of repeated usage. To evaluate the potential of repeated usage of immobilized cells, glass discs coated with *C. vulgaris* were washed thoroughly three times with culture media after toxicity testing. Subsequently, immobilized cells were either stored in nutrient media in the dark at 4 °C or cultured in a climate chamber at 20 °C under a light/dark cycle of 14/10 h according to the storing method described above. At regular intervals, short-term toxicity tests have been conducted. Before starting the toxicity tests, samples were washed and the vitality of the immobilized cells were evaluated by determining the quantum yield, $Y(I)_{prior\ exposure}$, of all samples before repeated exposure to the toxicant atrazine.

Results and discussion

Surface modification of the glass carrier for improved adherence of alginate hydrogels

In designing a cell-based detection system, the biocompatibility and stability of the immobilization matrix is important but so is

the attachment to the carrier substrate. In the present study, glass was chosen as carrier substrate due to its inertness and transparency. However, alginate gels did not remain attached to glass. Alginate films and dots easily slip down from unmodified glass. To overcome this, the surface of the glass was cationically modified. It has been shown that due to its negative charge, alginate forms strong complexes with polycations such as poly-L-lysine and poly(ethyleneimine). These complexes do not dissolve in the presence of Ca^{2+} chelators and are used to stabilize alginate gels.[21] The surface of the glass carriers was therefore cationically modified by dip coating using the polycation Catiofast 159. Alginate/silica hydrogel films and dots remained firmly attached to the modified glass surface even under fluid flow at 1000 rpm for about 3 months.

Catiofast 159-modified glass could be sterilized by autoclaving and stored in dry places for several months prior to use without losing its excellent adhering property for alginate. Surfaces other than glass, such as plastics, textiles and metals, can also be easily modified. For some carrier materials (glass and plastic), plasma treatment was necessary before polycation coating to ensure good surface wettability.

By choosing the kind of surface modification, the firmness of attachment but also the appearance of alginate dots (diameter and flatness) can be tuned depending on the hydrophobicity and polarity of the modified surface. With increasing hydrophobicity, the water-contact angle is elevated and alginate droplets spread less on the surface resulting in a decreased diameter of alginate dots. Thus, a closer center-to-center spacing of the dot array can be achieved on hydrophobic surfaces (see Fig. 1B). By contrast, a wider distance between each droplet has to be chosen for more hydrophilic surfaces to avoid merging of alginate spots.

Characterization of the amino-functionalized silica sol

Amino-functionalized silica sol used for gelation of sodium alginate was synthesized by mixing the silica precursor TEOS with diamino-functional silane and water. During hydrolysis reaction, alkoxide groups of the precursors were removed creating silanol groups (Si–OH) and releasing alcohol. Subsequent condensation reactions took place between silanol groups forming siloxane bonds (Si–O–Si) resulting in the
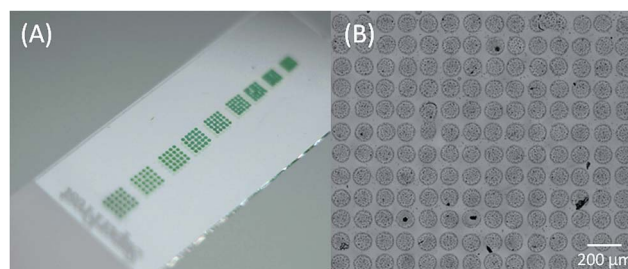

Fig. 1 (A) Alginate/silica arrays containing *C. vulgaris* cells printed onto Catiofast 159-modified glass slide with varying dot distance (ranging from 300 μm to 900 μm). Water contact angle about 15°. (B) Alginate array spotted onto a hydrophobic surface with a water contact angle of about 90° (dot distance 10 μm).

7900 | *J. Mater. Chem. B*, 2014, **2**, 7896–7909

This journal is © The Royal Society of Chemistry 2014

formation of silica nanoparticles bearing amino-groups. For a more detailed description of the principle of silica sol–gel synthesis for cell immobilization see Depagne et al.[13] or Pannier et al.[47] Alcohol formed during hydrolysis was removed by evaporation.

The FT-IR spectra of (A) unmodified silica sol and (B) amino-functionalized silica sol are shown in Fig. 2. The broad absorption band centred at about 3430 cm^{-1} can be attributed to the stretching of Si–OH groups presumably overlapped with the broad absorption band of adsorbed water. The strong and broad absorption band in the range of 1200–1000 cm^{-1} is most probably representing Si–O–Si groups which were formed as a result of the condensation reaction between silanol groups (Si–OH). The functionalization of the silica sol with amino groups is reflected by additional bands at about 2950 and 1470 cm^{-1} most likely representing vibrational modes of R–NH$_2$ functional groups and/or alkyl groups of the amino-functionalized silica.

Particle-size analysis demonstrated that amino-functionalized silica nanoparticles were in a range of 1–5 nm.

Characterization of alginate/silica hydrogels

The interactions of alginate with the amino-functionalized silica sol were investigated using FT-IR spectroscopy and SEM/EDX analysis. Fig. 2 shows the FT-IR spectra of (D) sodium alginate and (C) alginate/silica hydrogel. The FT-IR spectrum of Ca–alginate gels is not shown as it is quite identical to the spectrum of sodium alginate.

FT-IR spectra obtained in the present study are in accordance to Kurayama et al.[34] However, assignment of the absorption bands to specific functional groups is difficult due to the presence of bands related to residual water in the samples strongly interfering with bands of interest.

The FT-IR spectra of sodium alginate and alginate/silica hydrogel display characteristic bands observed for alginate. The broad peak near 3400 cm^{-1} indicates OH stretching vibrations of hydrogen-bonded OH groups. The two peaks near 1410 and 1600 cm^{-1} represent symmetric and asymmetric stretching vibrations of the COO$^-$, respectively, and the broad absorption

band in the 1200–1000 cm^{-1} region corresponds to vibrational modes of the carbohydrate ring. Only minor differences can be found between the spectra of the alginate/silica hydrogel (Fig. 2C) and sodium alginate (Fig. 2D). In the region between 1200 and 1000 cm^{-1} a slightly broader band is observed in the spectrum of alginate/silica hydrogel most probably representing the presence of Si–O–Si bonds. In addition, a weak band around 1450 cm^{-1} appeared which is tentatively assigned to the νs mode of carboxylate groups reflecting an increased number of these groups in this sample.

Previous studies showed that alginate may interact via electrostatic interactions with the amino-groups of polycations such as poly-L-lysine and chitosan.[48,49] In this way, the formation of alginate/silica hydrogels might be attributed to interactions between carboxyl groups of alginate and R–NH$_3^+$ groups of the amino-functionalized silica nanoparticles (see Fig. 3).[34,50,51] In addition to these interactions, alginate/silica hydrogels are presumably reinforced due to Si–O–Si bonds derived by the sol–gel process.[34,50,51]

To verify the incorporation of the silica nanoparticles within alginate/silica hydrogel films (gelation time 2 min), chemical composition was characterized by SEM-EDX analysis (data not shown). It was found that Si was present at the outer surface as well as at the interior of the films demonstrating that silica nanoparticles are able to penetrate the alginate network. By contrast, no Si was found for alginate films gelled by Ca^{2+}-ions.

When incubating droplets of 2% sodium alginate within the amino-functionalized silica sol (pH 7.5), it has been observed that the diameter of the alginate bead decreased significantly by about 35% within 20 min during incubation. Furthermore, the transparency of the beads was significantly reduced over time. Fig. 4 shows images of alginate/silica beads after different incubation times within the amino-functionalized silica sol. By contrast, shrinkage of the alginate bead was not so pronounced within 0.1 M CaCl$_2$ (about 15% within 20 min) and transparency was not so strongly affected over time of incubation. Similar findings have been observed by Kurayama et al.[34] They assigned the strong shrinkage of the alginate/silica hydrogel to aging processes of the amino-functionalized silica gel (condensation
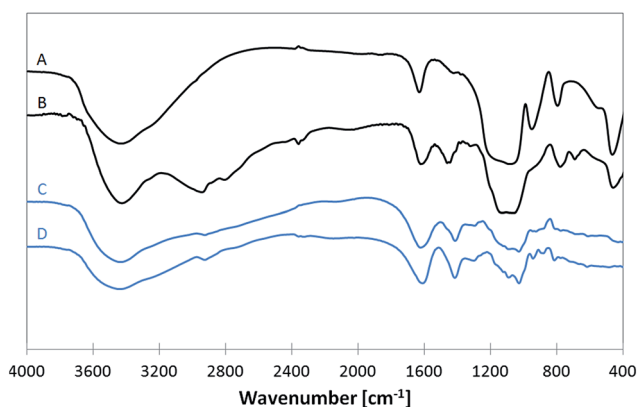

Fig. 2 FT-IR spectra of (A) unmodified silica sol, (B) amino-functionalized silica sol, (C) alginate/silica hydrogel and (D) sodium alginate. Spectra offset for clarity.
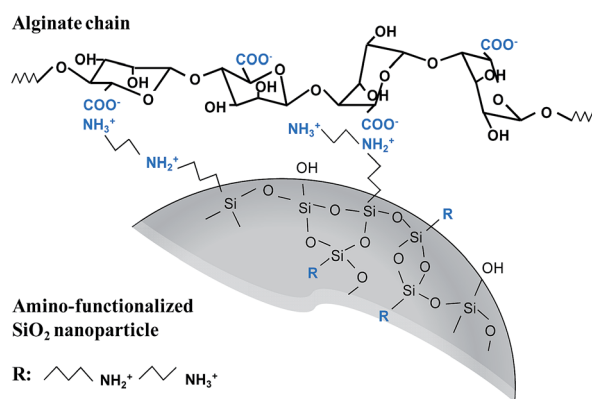

Fig. 3 Possible alginate/silica hydrogel formation due to interaction between amino groups of amino-functionalized silica and carboxyl groups of alginate.
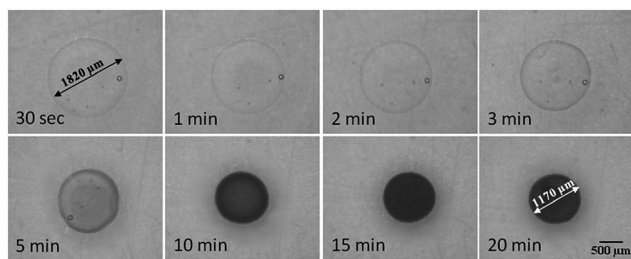
This journal is © The Royal Society of Chemistry 2014

J. Mater. Chem. B, 2014, 2, 7896–7909 | 7901

Fig. 4 Time course observation of an alginate bead during gelation reaction within amino-functionalized silica sol (pH 7.5).

of near Si–OH groups and formation of Si–O–Si bonds), as shrinkage increased with increasing initial concentration of the aminosilane and continues even though incorporation of the aminosilane was completed. Kurayama *et al.*[34] further observed that shrinkage of alginate is promoted under acidic and alkaline conditions as the pH significantly affects the dissociation of carboxyl groups and amino groups, as well as, the formation of Si–O–Si bonds *via* the sol–gel process.

Concerning transparency of alginate/silica hydrogel dots and films, pH 7.5 of the amino-functionalized silica sol gave best results. At that pH, carboxyl groups (–COO$^-$) of the repeating units of alginate dominate since carboxylic acid dissociation constants (pK_a) of 1,4-D-mannuronic acid (M) and α-L-guluronic acid (G) are 3.38 and 3.56, respectively.[49] Furthermore, considering the basic nature of amino groups of aminosilanes (pK_a is estimated at 9–10),[52,53] most of the amino groups of the amino-functionalized silica should be protonated.

For alginate/silica hydrogel films, a gelation time of 2 min has been chosen possessing best quality concerning transparency and stability. Due to the much smaller volume of printed alginate dot arrays (70 nL per dot) optimal contact time was reduced to 5 s. For longer contact times, an increasing opacity and a significant contraction of the small dots have been observed.

Stability testing

Ca–alginate matrices ionically gelled by conventional use of calcium ions (Ca^{2+}) are easily destabilized in the presence of Ca^{2+} chelators (*e.g.*, phosphates and citrates) and non-gelling agents such as Na$^+$. In the present study, alginate dots and films deposited onto Catiofast 159-modifed glass slides were gelled by amino-functionalized silica sol to improve matrix stability. The performance of the newly developed alginate/silica hybrid

Table 1 Stability testing of Ca–alginate and alginate/silica hydrogel dots within de-ionized water, phosphate buffer, 0.9% NaCl and culture medium over a period of two weeks ($-$ not stable, $\pm$ reasonably stable, $+$ stable)

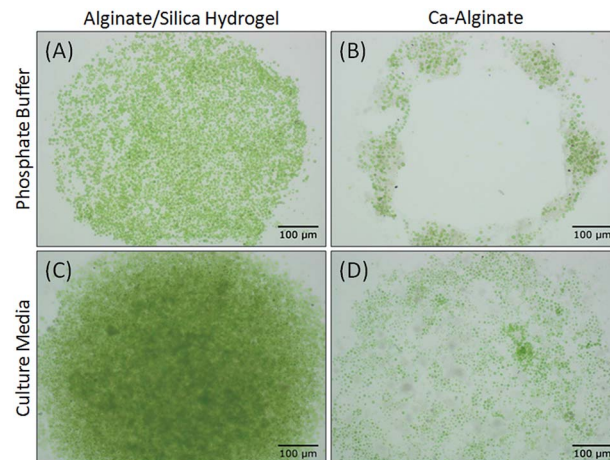|	dI-H$_2$O	PB	0.9% NaCl	1/2 Tamiya
Ca–alginate	+	−	−	±
Alginate/silica	+	+	+	+

Fig. 5 Light microscopy images of single (A and C) alginate/silica hydrogel dots and (B and D) Ca–alginate dots containing *C. vulgaris* cells (starting cell concentration 10^8 cells per mL sodium alginate). Dots were incubated (A and B) for 30 min in phosphate buffer (0.1 M PB, pH 7.0), and (C and D) for one week in 1/2 Tamiya culture medium at 20 °C under light/dark (14/10 h).

matrix was investigated in culture media (1/2 Tamiya) as well as in de-ionized water, phosphate buffer (PB) and 0.9% NaCl. Results were compared to Ca–alginate gels (see Table 1 and Fig. 5). Within de-ionized water, both gel matrices remained intact. However, Ca–alginate dots rapidly dissolved within phosphate buffer (0.1 M PB, pH 7.0) and physiological saline solution (0.9% NaCl). Only remnants of the Ca–alginate matrix could be found at the outer edge of the dots after 30 min incubation in phosphate buffer (see Fig. 5B). After longer exposure times, the remains of the Ca–alginate dots dissolved further. By contrast, alginate/silica hydrogel dots (see Fig. 5A) remained intact over a testing period of two weeks. Similar results were obtained with a physiological saline solution; but dissolution of Ca–alginate dots required slightly more time (about 20 h).

Within 1/2 Tamiya, Ca–alginate dots remained reasonably stable. However, Ca–alginate dots significantly swelled within the culture medium leading to strong cells leakage (Fig. 5D). After 1 week incubation in 1/2 Tamiya medium, only few cells remained within the Ca–alginate dots.

Alginate/silica hydrogel dots (Fig. 5C) also slightly swelled within the culture media but cell leakage was not so distinct and cells were retained within the gel matrix. Comparing Fig. 5A (corresponding to initial cell concentration) to Fig. 5C, where immobilized cells were incubated in culture media for one week, it can be seen that there was an increase of entrapped cell density during incubation in culture media. This finding indicates that the alginate/silica hydrogel is flexible enough to allow *C. vulgaris* cells to proliferate within the immobilization matrix.

Initial toxicity testing using fluorescence microscopy

Initial toxicity studies using the heavy metal ion copper demonstrated that algae entrapped within alginate/silica hydrogel dots can respond to their environment and changes in
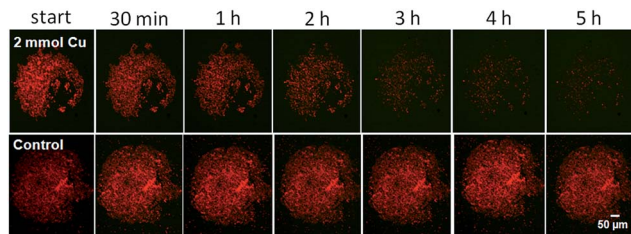
Fig. 6 Fluorescence images of a single dot of immobilized *C. vulgaris* cells after different periods of exposure time; (above) in the presence of 2 mmol copper-ions and (below) control without Cu. (Filter characteristics: Ex.: 460–490 nm; Em. > 520 nm; shutter speed 100 ms).

Chl *a* fluorescence can easily be observed (Fig. 6). At specific time intervals, cells were imaged using a fluorescence microscope. It can be seen that Chl *a* fluorescence decreased significantly in the presence of 2 mmol Cu over time. After 5 h, fluorescence was very weak. By contrast, control cells, which had not been in contact with copper ions showed little changes in fluorescence during that time. Due to the good responsiveness of *C. vulgaris* immobilized within the newly developed alginate/silica hydrogels, toxicity testing has been extended and the inhibition of photosynthesis was quantified by saturated pulse measurements using an imaging pulse-amplitude modulated chlorophyll fluorometer (Imaging-PAM) (see next Section).

Toxicity testing using PAM fluorometry

Short-term toxicity tests (exposure time: 1 h) have been conducted using the model herbicide atrazine. As the smallest adjustable area of interest (AOI) of the Imaging-PAM fluorometer was much bigger (2.08 mm) than the diameters of printed alginate/silica dots (650 μm), *C. vulgaris* cells were immobilized within thin films of alginate/silica hydrogels for toxicity testing. Immobilized cells have been exposed to six different concentrations of the model herbicide atrazine and the concentration–response curves were modelled based on the resulting inhibition of photosynthesis. For all samples, Chl *a* fluorescence was inhibited in a concentration dependent way and followed the sigmoidal concentration–response curve (example see Fig. 7). High correlation coefficients were obtained ($R^2 > 0.98$). For demonstrating the quality of experimental data sets behind the concentration–response curves and the goodness of statistical fits, the inhibition data of the sample demonstrating the highest variance of test results and the lowest R^2-value are visualized in Fig. 7.

In the following figures, only mean values of inhibition data are presented in order to simplify the presentation of data. Median effect concentrations (EC_{50}), which causes 50% inhibition of photosynthesis, are displayed in all figures for better evaluation of sample sensitivity and comparison to literature data. For more specified information and summary of all fitting parameters and statistical values, see ESI, Tables 2–5.†

Evaluation of sensitivities of immobilized *versus* suspended cells. To study whether the sensitivity of *C. vulgaris* cells to atrazine is modified by immobilization within alginate/silica
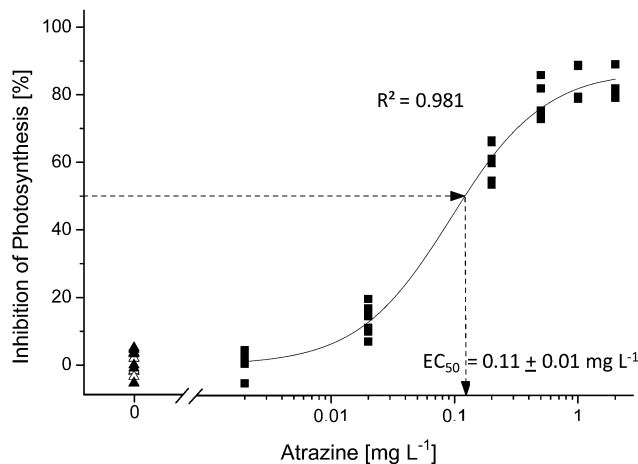

Fig. 7 Example of concentration–response curves modeled based on the measured inhibition data of photosynthesis in relation to controls ($N = 6$). Open triangles mark control samples without DSMO and filled triangles mark controls containing 0.1% of the solvent DSMO. EC_{50} denotes the concentration, which causes 50% inhibition of photosynthesis. (Here: test results are shown of samples stored 8 weeks at 20 °C; see Fig. 10B).

hydrogels, the response behaviour of immobilized *versus* freely suspended cells was monitored after selected exposure times to atrazine (1 h up to 24 h). Furthermore, the maximum quantum yield, $Y(I)$, of control samples (culture media with and without 0.1% DSMO) was compared to evaluate stress induced to the cells by immobilization (values see ESI, Table 2†). Short-term toxicity tests have been carried out the next day after immobilization. Samples have been stored at 25 °C in the dark in the meantime. After 1 h of illumination at about 40 μmol photons per m^2 s followed by 10 min dark adaptation, $Y(I)_{controls}$ was 0.41 ± 0.011 compared to 0.47 ± 0.005 for immobilized *versus* free cells; indicating minor effects on photosynthesis induced by immobilization.

Fig. 8 displays the concentration–response curves in the presence of atrazine. After 1 h of exposure, immobilized cells seemed to be only slightly more sensitive to that herbicide compared to freely suspended cells especially at higher toxicant concentrations, which may be due to stress induced by prior immobilization. The EC_{50} was 0.09 ± 0.007 mg L^{-1} compared to 0.11 ± 0.008 mg L^{-1}. However, differences were only minor. After 3 h exposure to the herbicide, differences were compensated and the concentration–response curves of immobilized and suspended cells showed a comparable response pattern.

Noteworthy, for both samples prolonged exposure times resulted in a decrease of inhibition of photosynthesis especially at high atrazine concentrations indicating physiological acclimation of the algae.[54,55] EC_{50} values were increased about three fold compared to starting conditions of 1 h exposure. Furthermore, the concentration–response curves reached saturation. For instance after 5 h exposure, a maximal response was reached at concentrations above 2 mg L^{-1} with approximately 90% of inhibition of photosynthesis for both, suspended and immobilized cells.
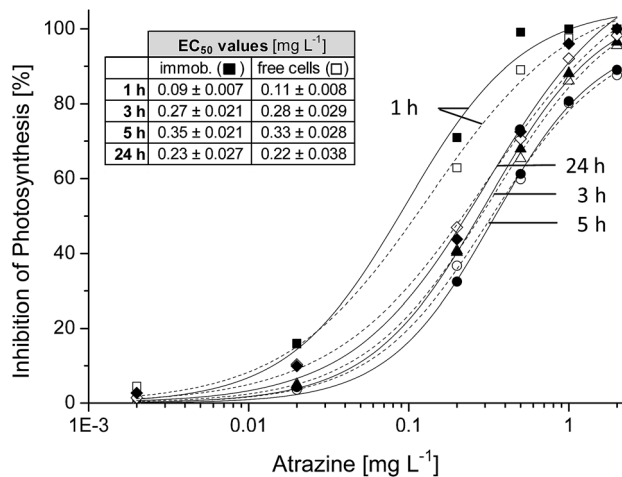
Fig. 8 Concentration–response curves of the inhibition of photosynthesis of immobilized (filled symbols and continuous lines) as well as freely suspended *C. vulgaris* cells (open symbols and dotted lines) after different exposure times to atrazine (1 h, 3 h, 5 h and 24 h). Mean values of inhibition data ($N = 6$) are presented.
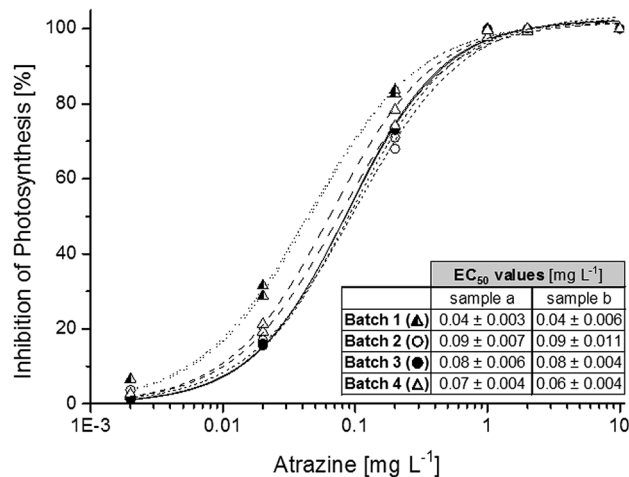

Fig. 9 Concentration–response curves of the inhibition of photosynthesis of independent batches of *C. vulgaris* cells immobilized within alginate/silica hydrogels (1 h exposure to atrazine). Mean values of inhibition data ($N = 6$) are presented.

After 24 h of exposure, inhibition of photosynthesis did again rise slightly. Compared to EC_{50} values after 1 h exposure, EC_{50} values were only twice as high. The increase in sensitivity may be due to secondary effects of the herbicide (inhibition of repair mechanisms and rapid chlorophyll turnover).[56] For the following experiments exposure of 1 h has been chosen, possessing the highest sensitivity.

EC_{50} values obtained in the present study showed good correspondence to literature data. From the ECOTOX-database of the US EPA (June 06, 2014),[57] EC_{50} values for photosynthesis could be retrieved for atrazine in the range of 0.06–0.15 mg L^{-1} for *C. vulgaris*[1,39,58,59] and 0.03–0.5 mg L^{-1} for other species of *Chlorella*[41,60–62] (exposure times ranging from 5 min to 3 h).

Evaluation of reproducibility. Reproducibility of the response pattern was evaluated between four independent batches of immobilization. Over a period of two months, samples of *C. vulgaris* cells in batch culture were harvested for immobilization at four independent time intervals.

24 hours after cell immobilization within thin layers of alginate/silica hydrogel films, short-term toxicity tests were conducted (1 h exposure to atrazine). Fig. 9 depicts the concentration–response curves obtained for four independent batches. It can be seen that concentration–response curves obtained for samples from the same batch (samples a and b in Fig. 9) showed excellent correspondence. Between immobilized cells derived from different batches, minor differences in the concentration-dependent responses could be observed. EC_{50} values derived from independent batches varied by a factor of two only (ranging from 0.04 mg L^{-1} to 0.09 mg L^{-1}), still demonstrating an adequate correspondence. Differences are probably due to test variance and biological variability. Similar results (variance by a factor of two between parallel and independent batches) have been obtained by Faust *et al.*[63] who investigated the reproducibility of algal toxicity tests using synchronized cultures of suspended *Chlorella* sp. Védrine *et al.*[39]

demonstrated that the reproducibility could be improved by continuous cultivation techniques to provide cells in the same physiological state for immobilization and toxicity tests.

Evaluation of storage stability. To detect the influence of age and storage conditions of *C. vulgaris* cells immobilized within alginate/silica hydrogels, short-term toxicity tests were performed after storage at 4 °C (in the dark) and at 20 °C (light/dark cycle of 14/10 h). After specific periods of storage (up to 8 weeks), immobilized cells were thoroughly washed before exposure to atrazine to eliminate suspended cells. Fig. 10 depicts the age-dependent concentration–response curves and EC_{50} values evaluated after 1 h exposure to atrazine. It can be seen that after storage at 4 °C in the dark (Fig. 10A), concentration–response curves showed good correspondence to starting conditions (continuous line in Fig. 7A) especially for concentrations <1 mg L^{-1}. EC_{50} values remained in the range of initial data, indicating that older samples were almost as sensitive to atrazine as freshly immobilized cells. After 8 weeks of storage at 4 °C, no complete inhibition of photosynthesis was achieved at elevated test concentrations. Maximal inhibition A_{max} was about 94%.

Samples stored at 20 °C (Fig. 10B) showed good correspondence after 1 and 2 weeks of storage compared to newly immobilized samples. For longer storage periods, a shift in sensitivity can be observed. Samples stored at 20 °C for 4 weeks and longer seemed to be less sensitive to atrazine. EC_{50} values were increased by a factor of three up to 0.12 compared to starting conditions (EC_{50} 0.04). However, EC_{50} values were still comparable to literature date from ECOTOX-database where values ranging from 0.06–0.15 mg L^{-1} were found for *C. vulgaris*[1,39,58,59] as previously discussed.

The decrease in sensitivity over time of storage may be due to proliferation and aging of the immobilized cells. These results are consistent with those of Ivorra *et al.*[69] and Schmitt-Jansen *et al.*[41] They observed a decrease in sensitivity to atrazine and
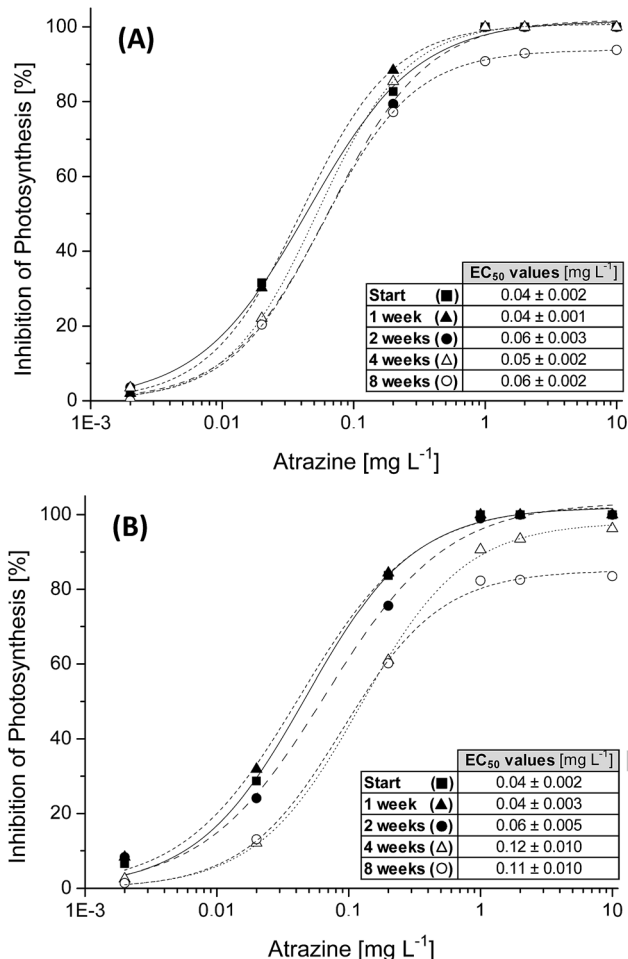
Fig. 10 Age-dependent concentration–response curves of the inhibition of photosynthesis after storage (A) at 4 °C in the dark or (B) at 20 °C under a light/dark cycle of 14/10 h in culture media. Exposure time 1 h. Mean values of inhibition data (N = 6) are presented.
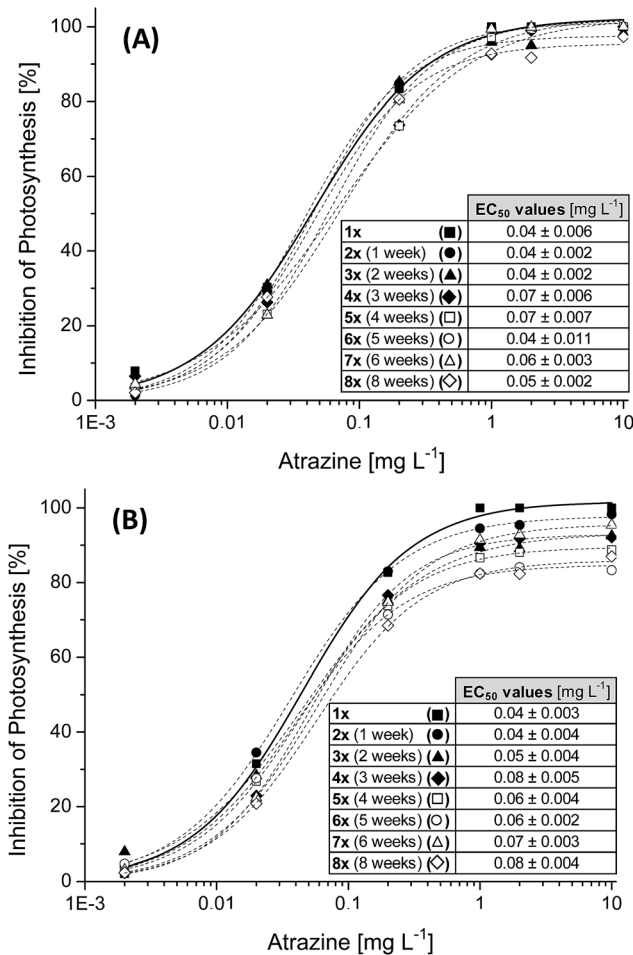

Fig. 11 Concentration–response curves after repeated-usage. After each exposure cycle, immobilized cells were washed vigorously and transferred to fresh culture media. Samples were either (A) stored at 4 °C in the dark or (B) cultured at 20 °C under a light/dark cycle of 14/10 h until the next exposure cycle. Age of the samples is given in parenthesis. Periods of intermediate storage were one week for cycles 1–7 and two weeks between cycle 7 and 8. Concentration–response curves of the first exposure are marked with continuous lines. Exposure time 1 h. Mean values of inhibition data (N = 6) are presented.

other herbicides for older microalgal biofilms which correlated with growth and biomass.

Comparing $Y(I)$ values of control samples (see ESI, Table 4†), it can be seen that $Y(I)_{controls}$ rises from 0.39 to about 0.52 over time of storage under cultivation conditions at 20 °C. This finding indicates recovery of the *C. vulgaris* cells from possible stress induced by the immobilization procedure but also cell growth within the alginate/silica hydrogel.

By contrast, after a first slight increase after one week storage at 4 °C from 0.39 to 0.43 (probably due to cell recovery), $Y(I)_{controls}$ values stayed constant for the whole storage period investigated (8 weeks).

Evaluation of repeated usage. Being non-invasive, the *in vivo* observation of Chl *a* fluorescence by Imaging-PAM provides the possibility to regenerate and reuse the designed cell-based detection system. To assess the potential of repeated usage, eight exposure cycles were conducted with intermediate storage and regeneration of immobilized cells for 1 week between each cycle in culture media.

Immobilized cells were washed vigorously with water after each exposure and transferred to fresh culture media. Two

different possibilities of intermediate storage between each cycle have been investigated. Samples were either stored at 4 °C in the dark or cultured at 20 °C under illumination (14/10 h light/dark cycle). Culture media were exchanged daily to avoid nutrient depletion. Every week repeated toxicity tests were carried out. For validation of recovery and vitality of repeatedly used cells, samples were washed rigorously to remove free cells, transferred to fresh media containing no atrazine, and $Y(I)$ was measured for each sample prior to each exposure cycle. Mean values of $Y(I)_{prior\ exposure}$ can be found in ESI, Table 5.† In general, no significant variations were observed between samples previously exposed to atrazine (concentrations ranging from 0.002–10 mg L^{-1}) and control samples which were never in contact with that herbicide. This finding indicates that inhibition of photosynthesis by atrazine is reversible and *C. vulgaris* cells immobilized within alginate/silica hydrogels are able to recover from short-term exposure to atrazine. In accordance to

the results of the previous experiment (evaluation of storage stability; see Fig. 10 and ESI, Table 4†), where samples were never exposed to atrazine, similar findings were observed when comparing mean values of $Y(I)_{prior\ exposure}$ for each exposure cycle. During intermediate storage under cultivation conditions at 20 °C, there was an increase in $Y(I)_{prior\ exposure}$ indicating cell growth. For samples stored intermediately at 4 °C in the dark, this shift was much lower. However, as cells were repeatedly exposed to light and 20 °C during exposure cycles, the increase in $Y(I)_{prior\ exposure}$ was higher compared to the previous experiment where samples were continuously stored in the dark at 4 °C prior to toxicity testing.

Repeatedly conducted short-term exposure tests (Fig. 11) demonstrated that compared to starting conditions, repeatedly exposed cells showed in general a similar sensitivity to atrazine after recovery; especially when stored at 4 °C (Fig. 11A). The good agreement of the concentration–response curves demonstrates clear stability and reversibility of the concentration-dependent response of immobilized cells. C. vulgaris cells immobilized within alginate/silica hydrogels were able to recover readily from the inhibitory effects of atrazine after repeated usage. The results of this study suggest that even after intermediate storage at ambient temperatures (20 °C) between each exposure cycle (Fig. 11B), correspondence of the response pattern was achieved. However, at elevated concentrations no complete inhibition of the PSII was achieved after repeated exposure to atrazine, indicating tolerance development. With rising number of exposure cycles and age of the immobilized cells, maximal inhibition A_{max} showed a tendency to decrease.

The adaptation to herbicide exposure by developing tolerances is a common feature. For instance, microalgae cells exposed to atrazine were revealed to be less affected by additional atrazine than were previously unexposed cells.[64,65] This phenomenon was not so distinctive when samples were stored under cool conditions in the dark indicating a dependency of the effect from growth and an active photosystem during light exposure.

Thus storage under cool conditions seemed favourable in avoiding cell proliferation and minimizing aging effects. EC_{50} values were achieved ranging from 0.04 to 0.07 mg L^{-1} even after 8 weeks of storage at 4 °C. Nevertheless, a comparable sensitivity is also obtained for samples stored at 20 °C for about 2 weeks with EC_{50} ranging from 0.04 to 0.06 mg L^{-1}. For older samples a more pronounced shift in sensitivity has been observed. However, EC_{50} values were still in the range of data retrieved from ECOTOX-database.

Besides the good results of the performance of C. vulgaris cells during repeated short-term toxicity tests, it has to be taken into account that results have to be seen in correlation to the triazine herbicide atrazine. This herbicide generally produces a reversible inhibition of the PSII. It is barely bioaccumulated and typically does not result in lethality or permanent cell damage in short term.[66] The performance of the designed cell-based detection system may thus be different in the presence of other toxicants.

Rapid recovery of algae has also been reported for photosynthesis inhibitors other than atrazine[67,68] Reversibility and possibility to re-use immobilized algal cells for toxicity tests were shown for atrazine and other triazine herbicides (e.g., simazine, propazine, terbuthylazine) as well as urea based herbicides (e.g., isoproturon, diuron, linuron).[3,39,59] By contrast, the phenolic herbicide dinitro-o-cerosol (DNOC) produced irreversible damage to C. vulgaris cells due to uncoupling effects of oxidative phosphorylation in addition to the inhibition of PSII electron transport.[39]

Comparison of the results of repeatedly used samples to the previous experiment where the storage stability has been evaluated, demonstrated that in both cases the response signal to atrazine remained largely preserved after storage for up to 8 weeks even when the samples were repeatedly exposed to short-term toxicity tests.

EC_{50} values obtained after storage with and without repeated usages were still in the same range as results obtained between independent batches (see section Evaluation of reproducibility) thereby confirming the work of Baxter et al.,[68] who found that the sensitivity of Pseudokirchneriella subcapitata populations does not change by pulsed previous exposures with atrazine.

Only samples stored at 20 °C under a light/dark cycle, showed a more pronounced shift in sensitivity; EC_{50} rises up to 0.08 mg L^{-1}. Never exposed samples of the previous storage experiment even showed a more significant shift in sensitivity where EC_{50} rises up to 0.12 mg L^{-1} after 4 weeks of storage. The reason for the lower sensitivity of previously unexposed samples could be that these samples were not disturbed during cell growth. The resulting denser colonies could shade the inhibition of photosynthesis more intensely.

Whereas at low test concentrations, never exposed samples demonstrated less sensitivity to atrazine, at elevated concentrations a more pronounced tolerance development was observed for repeatedly exposed samples with no complete inhibition of photosynthesis at elevated test concentrations. Whereas the maximal inhibition of the 4 weeks old never exposed samples reached almost maximum (A_{max} = 98.7%), A_{max} was 89.5% for repeatedly used samples. After 8 weeks of storage at 20 °C, previously unexposed samples showed a comparable sensitivity to repeatedly exposed samples at elevated atrazine concentration.

Conclusion

The first objective of this study was to firmly immobilize living cells within patterned cell arrays by printing techniques. Arrays of single dots of a sodium alginate/cell suspension were therefore printed onto cationically-modified glass carriers. By immersion within amino-functionalized silica sol, deposited spots were gelled within seconds directly after printing. In addition to the fast gelation and the ease of printing, this approach presented the possibility to significantly reinforce alginate gels. Compared to alginate gels ionically cross-linked using conventional Ca^{2+}-ions, the newly developed alginate/silica hydrogels showed improved stability in saline solutions. The cationic ammonium groups of the organically modified silica sols seem to be able to interact strongly with the anionic groups of the alginate. By condensation reactions between

amino-functionalized silica nanoparticles a silica gel network may form, further reinforcing the alginate/silica hybrid matrix.

In contrast to pure silica hydrogels where cells are commonly unable to divide within the rigid silica matrix and may thus be physiologically compromised,[13,70] C. vulgaris cells were able to grow and divide within the alginate/silica hydrogel matrix. This fact may favour the long-term viability and activity of the immobilized cells observed in the present study.

The second aim of this study was to investigate the applicability of alginate/silica hydrogels as immobilization matrix for the design of cell-based detection systems. Short-term toxicity tests (exposure time 1 h) using the herbicide atrazine as model toxicant and the green microalgae C. vulgaris as sensing microorganism demonstrated that C. vulgaris cells immobilized within alginate/silica hydrogels remain capable of reporting the presence of that toxicant. Photosynthetic activity has been evaluated by measuring changes in Chl a fluorescence using PAM-fluorometry. The response of the immobilized microalgae was concentration-dependent and rapid and could be compared to freely suspended cells. The evaluation of the reproducibility by comparing sensitivities between parallel and independent batches of immobilized cells showed reasonable response variability.

The presented study demonstrated that the photosynthetic activity and response sensitivity to atrazine of C. vulgaris immobilized within alginate/silica hydrogels was maintained over several weeks. Cells could thus be easily stored and transported after immobilization allowing operation in the field. Furthermore, immobilized C. vulgaris cells could be repeatedly used for short-term toxicity tests. Response characteristics of the sensing cells to atrazine revealed to be reversible and largely preserved for up to 8 weeks after immobilization and several cycles of repeated usage. Storage under cool conditions in the dark is favourable compared to storage at 20 °C under light/dark cycles.

Nevertheless, results have to be considered confined to atrazine and other triazines as they induce no permanent cell damage in the short-term and inhibition of photosynthesis is completely reversible.

Although this study centred on the microalgae C. vulgaris, preliminary studies of other cell types were also performed; for instance the microalgal strain Kirchneriella contorta, as well as Gram-positive (Bacillus subtilis) and Gram-negative (Escherichia coli) bacteria, and yeast cells (Saccharomyces cerevisiae) were immobilized within alginate/silica hydrogels. They also remained viable upon immobilization and were able to proliferate within the gel matrix. Thus, immobilization of microorganisms within alginate/silica hydrogels may be suitable for the design of multispecies test systems.

Perspectives

In view of their high stability in saline solutions and their firm attachment to cationically-modified glass carriers, alginate/silica hydrogels demonstrate high potential for use in the design of cell-based detection systems. By printing processes, multiple cell arrays may be created.

Due to limitations of the applied Imaging-PAM fluorometer in downsizing the area used for Chl a fluorescence measurements in the present study, C. vulgaris cells were immobilized within thin films of alginate/silica hydrogels by dip coating and not by printing. In order to fully use the potential of printing cell arrays, future work is planned to apply a Microscopy-PAM fluorometer (HeinzWalz GmbH, Effentrich, Germany). By combining a PAM-fluorometer with an inverted epifluorescence microscope high spatial resolution can be achieved, which allows the detection of fluorescence signals of single cells.

Future work is planned to immobilize different microalgae strains of different groups (e.g., chlorophytes, cyanophytes and diatoms) onto a single support in order to test the potential of the printing process to generate multispecies test systems. Therefore, multiple algal strains shall be immobilized each in separate dots and its performance during toxicity testing and storage shall be evaluated. Taking advantage of the different response sensitivities, this approach could be a promising tool for a fast evaluation of the ecotoxicological state of environmental samples.

Notes and references

1 B. Podola and M. Melkonian, J. Appl. Phycol., 2005, 17(3), 261–271.

2 M. Altamirano, L. García-Villada, M. Agrelo, L. Sánchez-Martín, L. Martín-Otero, A. Flores-Moya, M. Rico, V. López-Rodas and E. Costas, Biosens. Bioelectron., 2004, 19(10), 1319–1323.

3 E. Peña-Vázquez, E. Maneiro, C. Pérez-Conde, M. C. Moreno-Bondi and E. Costas, Biosens. Bioelectron., 2009, 24(12), 3538–3543.

4 H. Ben-Yoav, S. Melamed, A. Freeman, Y. Shacham-Diamand and S. Belkin, Crit. Rev. Biotechnol., 2011, 31(4), 337–353.

5 S. Melamed, T. Elad and S. Belkin, Anal. Biotechnol., 2012, 23(1), 2–8.

6 R. S. Kane, S. Takayama, E. Ostuni, D. E. Ingber and G. M. Whitesides, Biomaterials, 1999, 20(23–24), 2363–2376.

This journal is © The Royal Society of Chemistry 2014

J. Mater. Chem. B, 2014, 2, 7896–7909 | 7907

7 D. Falconnet, G. Csucs, H. Michelle Grandin and M. Textor, *Biomaterials*, 2006, **27**(16), 3044–3063.

8 O. Berthuy, C. Mandon, B. Corgier, G. Octobre, G. Ceccone, V. Spampinato, L. Blum and C. Marquette, *J. Mater. Sci.*, 2014, **49**(13), 4481–4489.

9 E. A. Roth, T. Xu, M. Das, C. Gregory, J. J. Hickman and T. Boland, *Biomaterials*, 2004, **25**(17), 3707–3715.

10 T. G. Fernandes, S.-J. Kwon, M.-Y. Lee, D. S. Clark, J. M. S. Cabral and J. S. Dordick, *Anal. Chem.*, 2008, **80**(17), 6633–6639.

11 L. Xu, L. Robert, Q. Ouyang, F. Taddei, Y. Chen, A. B. Lindner and D. Baigl, *Nano Lett.*, 2007, **7**(7), 2068–2072.

12 S. Melamed, L. Ceriotti, W. Weigel, F. Rossi, P. Colpo and S. Belkin, *Lab Chip*, 2011, **11**(1), 139–146.

13 C. Depagne, C. Roux and T. Coradin, *Anal. Bioanal. Chem.*, 2011, **400**(4), 965–976.

14 E. J. Cho, Z. Tao, E. C. Tehan and F. V. Bright, *Anal. Chem.*, 2002, **74**(24), 6177–6184.

15 N. Rupcich, A. Goldstein and J. D. Brennan, *Chem. Mater.*, 2003, **15**(9), 1803–1811.

16 M. R. N. Monton, E. M. Forsberg and J. D. Brennan, *Chem. Mater.*, 2011, **24**(5), 796–811.

17 X. Ge, J. M. Lebert, M. R. N. Monton, L. L. Lautens and J. D. Brennan, *Chem. Mater.*, 2011, **23**(16), 3685–3691.

18 H. K. Baca, E. Carnes, S. Singh, C. Ashley, D. Lopez and C. J. Brinker, *Acc. Chem. Res.*, 2007, **40**(9), 836–845.

19 X. Ge, N. M. Eleftheriou, S. A. Dahoumane and J. D. Brennan, *Anal. Chem.*, 2013, **85**(24), 12108–12117.

20 J. M. Lebert, E. M. Forsberg and J. D. Brennan, *Biochem. Cell Biol.*, 2008, **86**, 100–110.

21 W. R. Gombotz and S. Wee, *Peptide Release from Polymer Matrices*, 1998, **31**(3), 267–285.

22 Ý. A. Mørch, I. Donati and B. L. Strand, *Biomacromolecules*, 2006, **7**(5), 1471–1480.

23 I. Moreno-Garrido, *Bioresour. Technol.*, 2008, **99**(10), 3949–3964.

24 T. Coradin in *Nanocomposites with biodegradable polymers: Synthesis, properties, and future perspectives*, ed. V. Mittal, Oxford University Press, Oxford, New York, 2011.

25 M. Perullini, M. Jobbágy, N. Mouso, F. Forchiassin and S. A. Bilmes, *J. Mater. Chem.*, 2010, **20**(31), 6479–6483.

26 B. Thu, P. Bruheim, T. Espevik, O. Smidsrød, P. Soon-Shiong and G. Skjåk-Bræk, *Biomaterials*, 1996, **17**(10), 1031–1040.

27 S. Birnbaum, R. Pendleton, P.-O. Larsson and K. Mosbach, *Biotechnol. Lett.*, 1981, **3**(8), 393–400.

28 M. Perullini, M. Jobbágy, G. J. A. A. Soler-Illia and S. A. Bilmes, *Chem. Mater.*, 2005, **17**(15), 3806–3808.

29 Y. Fukushima, K. Okamura, K. Imai and H. Motai, *Biotechnol. Bioeng.*, 1988, **32**(5), 584–594.

30 Y. Ferro, M. Perullini, M. Jobbágy, S. A. Bilmes and C. Durrieu, *Sensors*, 2012, **12**(12), 16879–16891.

31 M. Perullini, Y. Ferro, C. Durrieu, M. Jobbágy and S. A. Bilmes, *J. Biotechnol.*, 2014, **179**(0), 65–70.

32 T. Coradin, E. Mercey, L. Lisnard and J. Livage, *Chem. Commun.*, 2001, (23), 2496–2497.

33 S. Sakai, T. Ono, H. Ijima and K. Kawakami, *Biomaterials*, 2001, **22**(21), 2827–2834.

34 F. Kurayama, S. Suzuki, T. Oyamada, T. Furusawa, M. Sato and N. Suzuki, *J. Colloid Interface Sci.*, 2010, **349**(1), 70–76.

35 R. Brayner, A. Couté, J. Livage, C. Perrette and C. Sicard, *Anal. Bioanal. Chem.*, 2011, **401**(2), 581–597.

36 H. Nguyen-Ngoc, C. Durrieu and C. Tran-Minh, *Ecotoxicol. Environ. Saf.*, 2009, **72**(2), 316–320.

37 C. Durrieu and C. Tran-Minh, *Ecotoxicol. Environ. Saf.*, 2002, **51**(3), 206–209.

38 E. Peña-Vázquez, C. Pérez-Conde, E. Costas and M. C. Moreno-Bondi, *Ecotoxicology*, 2010, **19**(6), 1059–1065.

39 C. Védrine, J.-C. Leclerc, C. Durrieu and C. Tran-Minh, *Biosens. Bioelectron.*, 2003, **18**(4), 457–463.

40 W. Draber, K. Tietjen, J. F. Kluth and A. Trebst, *Angew. Chem., Int. Ed. Engl.*, 1991, **30**(12), 1621–1633.

41 M. Schmitt-Jansen and R. Altenburger, *Toxicol. Environ. Chem.*, 2007, **89**(4), 665–681.

42 U. Schreiber, in *Chlorophyll a Fluorescence*, ed. G. Papageorgiou and Govindjee, Springer, Netherlands, 2004, 279–319.

43 E. Hase, Y. Morimura and H. Tamiya, *Arch. Biochem. Biophys.*, 1957, **69**(0), 149–165.

44 M. Gepp, F. Ehrhart, S. Shirley, S. Howitz and H. Zimmermann, *Biotechnol.*, 2009, **46**(1), 31–43.

45 B. Genty, J.-M. Briantais and N. R. Baker, *Biochim. Biophys. Acta, Gen. Subj.*, 1989, **990**(1), 87–92.

46 J. C. Kromkamp and R. M. Forster, *Eur. J. Phycol.*, 2003, **38**(2), 103–112.

47 A. Pannier and U. Soltmann, in *Advances in Materials Science Research: vol. 12*, Nova, Science Publishers, New York, 2012, 49–88.

48 S. K. Tam, J. Dusseault, S. Polizu, M. Ménard, J.-P. Hallé and L. Yahia, *Biomaterials*, 2005, **26**(34), 6950–6961.

49 G. Lawrie, I. Keen, B. Drew, A. Chandler-Temple, L. Rintoul, P. Fredericks and L. Grøndahl, *Biomacromolecules*, 2007, **8**(8), 2533–2541.

50 H. Wu, Y. Zhao, M. Nie and Z. Jiang, *Sep. Purif. Technol.*, 2009, **68**(1), 97–104.

51 W. Zhang, S. He, Y. Liu, Q. Geng, G. Ding, M. Guo, Y. Deng, J. Zhu, J. Li and Y. Cao, *ACS Appl. Mater. Interfaces*, 2014, **6**(14), 11783–11790.

52 T. Yokoi, Y. Kubota and T. Tatsumi, *Appl. Catal., A*, 2012, **421–422**(0), 14–37.

53 E. Metwalli, D. Haines, O. Becker, S. Conzone and C. G. Pantano, *J. Colloid Interface Sci.*, 2006, **298**(2), 825–831.

54 F. Marvá, V. López-Rodas, M. Rouco, M. Navarro, F. J. Toro, E. Costas and A. Flores-Moya, *Aquat. Toxicol.*, 2010, **96**(2), 130–134.

55 A. D. Bradshaw and K. Hardwick, *Biol. J. Linn. Soc.*, 1989, **37**(1–2), 137–155.

56 H. Nestler, K. J. Groh, R. Schönenberger, R. Behra, K. Schirmer, R. I. L. Eggen and M. J.-F. Suter, *Aquat. Toxicol.*, 2012, **110–111**, 214–224.

57 U.S. Environmental Protection Agency, *ECOTOX User Guide: ECOTOXicology Database System*, 4th edn, 2013, http://www.epa.gov/ecotox/, update 2014/06/06.

58 R. Muller, U. Schreiber, B. I. Escher, P. Quayle, S. M. Bengtson Nash and J. F. Mueller, *Sci. Total Environ.*, 2008, **401**(1–3), 51–59.

59 M. Naessens, J. C. Leclerc and C. Tran-Minh, *Ecotoxicol. Environ. Saf.*, 2000, **46**(2), 181–185.

60 R. Altenburger, W. Bödeker, M. Faust and L. Horst Grimme, *Ecotoxicol. Environ. Saf.*, 1990, **20**(1), 98–114.

61 G. Stratton, *Arch. Environ. Contam. Toxicol.*, 1984, **13**(1), 35–42.

62 C. M. Hersh and W. G. Crumpton, *Environ. Toxicol. Chem.*, 1989, **8**(4), 327–332.

63 M. Faust, R. Altenburger, W. Bödeker and L. H. Grimme, *Schr.-Reihe Verein WaBoLu*, 1992, **89**, 311–321.

64 M. Schmitt-Jansen and R. Altenburger, *Environ. Toxicol. Chem.*, 2005, **24**(2), 304–312.

65 B. Nyström, M. Paulsson, K. Almgren and H. Blank, *Environ. Toxicol. Chem.*, 2000, **19**(5), 1324–1331.

66 K. R. Solomon, D. B. Baker, R. P. Richards, K. R. Dixon, S. J. Klaine, T. W. La Point, R. J. Kendall, C. P. Weisskopf, J. M. Giddings, J. P. Giesy, L. W. Hall and W. M. Williams, *Environ. Toxicol. Chem.*, 1996, **15**(1), 31–76.

67 R. A. Brain, J. R. Arnie, J. R. Porch and A. J. Hosmer, *Environ. Toxicol. Chem.*, 2012, **31**(11), 2572–2581.

68 L. Baxter, R. Brain, R. Prosser, K. Solomon and M. Hanson, *Environ. Pollut.*, 2013, **181**, 325–328.

69 N. Ivorra, S. Bremer, H. Guasch, M. H. S. Kraak and W. Admiraal, *Environ. Toxicol. Chem.*, 2000, **19**(5), 1332–1339.

70 N. M. Eleftheriou, X. Ge, J. Kolesnik, S. B. Falconer, R. J. Harris, C. Khursigara, E. D. Brown and J. D. Brennan, *Chem. Mater.*, 2013, **25**(23), 4798–4805.